**Educational Administration: Theory and Practice**
2024, 30(6), 259-267
ISSN: 2148-2403
https://kuey.net/

**Research Article**

# Mapping Sowing Dates of Paddy in Different Agro-Climatic Regions of Punjab using SAR Satellite Data

Parmod Kumar[1*], Rajesh Jolly [1], Ripudaman Singh [2]

[1*]Lovely Professional University Phagwara, Punjab, parmod.nehra25@gmail.com, rajesh.26775@lpu.co.in,
[2]Amity University, Noida, Uttar Pradesh, ripudaman1@gmail.com

***Citation:*** Parmod Kumar et al. (2024), Mapping Sowing Dates of Paddy in Different Agro-Climatic Regions Of Punjab Using SAR Satellite Data Educational *Administration: Theory And Practice*, *30* (6), 259-267
Doi: 10.53555/kuey.v30i6.5160

**ARTICLEINO**

**ABSTRACT**

Rice is a major staple crop in the world, and therefore, accurate acreage assessment of crop area is essential. Traditional methods of crop acreage estimation often rely on ground surveys and manual data collection, which are labor intensive, time-consuming, and may lack spatial coverage. In recent years, the availability of satellite remote sensing data has revolutionized the monitoring of agricultural systems by providing frequent, spatially extensive, and cost-effective information. This study presents a remote sensing approach for assessing crop area and identifying sowing dates using satellite data. We used the Sentinel-1 synthetic aperture radar (SAR) data to estimate the acreage of rice crop and sowing/transplanting of kharif rice during the years 2019 & 2020. Results showed that the rice area and sowing dates were validated using ground truth, and an overall accuracy of 87 to 92% was achieved for both years. Satellite based assessment of crop area and sowing date identification provides reliable information with high spatial and temporal resolution, enabling timely decision-making for farmers, policymakers, and agricultural stakeholders. Furthermore, the scalability and cost-effectiveness of satellite remote sensing make it a valuable tool for large-scale agricultural monitoring and management. In conclusion, this study highlights the potential of Sentinel-1 SAR satellite data for early-stage assessment of rice crop areas, offering a practical and efficient solution for monitoring agricultural dynamics at regional and global scales. Continued advancements in satellite technology and data processing techniques promise further improvements in the accuracy and applicability of remote sensing-based approaches for agricultural monitoring and management.

**Keywords**: Rice, synthetic aperture radar, remote sensing

## Introduction

Rice (Oryza sativa L.) is a chief staple food crop in the world, cultivated in various regions under different climatic conditions, ranging from areas of high rainfall to the driest deserts with the aid of irrigation. Rice occupies an extraordinarily large portion of the total cropped area in South, Southeast, and East Asia. Rice cultivation is a crucial socio-economic driving factor in developing Asian countries, where over 90% of the world's rice is produced and consumed (Laborte et al., 2017). In India, rice is one of the major kharif crops, mainly grown in 14 states, with Punjab being one of the largest rice-producing states, producing approximately 11 million tonnes of rice (Government of India, 2019). Extreme abiotic conditions such as high temperatures, droughts, salinity, severe rains, and floods pose serious hazards to rice production due to global climate change. Additionally, rice cultivation is strongly related to environmental issues such as water consumption and greenhouse gas emissions. Inundated rice fields, in particular, are a significant source of methane, accounting for 25% of the global methane emissions from agriculture (1996 IPCC). To address these issues, long-term rice monitoring becomes increasingly important at both global and farm levels. Conventional methods like field survey techniques for collecting crop statistics are time-consuming and laborious.
ed rice fields, in particular, are a significant source of methane, accounting for 25% of the global methane emissions from agriculture (1996 IPCC). To address these issues, long-term rice monitoring becomes

increasingly important at both global and farm levels. Conventional methods like field survey techniques for collecting crop statistics are time-consuming and laborious.

Remote sensing permits repetitive coverage, which is useful for gathering information on dynamic themes such as water and agricultural fields. It allows for the straightforward collection of data over various scales and resolutions. Satellite remote sensing has become an important tool for crop monitoring (Sishodia et al., 2020; Chen et al., 2021), with optical remote sensing being used for comprehensive monitoring of relevant parameters during the rice growing period. Crop classification and the discriminant function are determined according to crop characteristics, including brightness, hue, position, texture, and structure. However, optical remote sensing data is often affected by severe weather conditions such as clouds, rain, and fog. For instance, cloudiness and frequent rains in mountainous or watershed areas make it difficult to obtain suitable images to study the rice-growing season. Additionally, optical images may contain similar objects with different spectra and different objects with similar spectra, presenting limitations in identifying and monitoring rice and other crops. Synthetic aperture radar (SAR) has the capability of high resolution, multi-mode, multi-polarization, all-weather acquisition, and sensitivity to surface moisture, material, and surface roughness, which compensates for the deficiencies of optical data, especially during the monsoon season (Boschetti et al., 2017; Liu et al., 2019; Ulaby et al., 1986). Rice exhibits a substantially larger time-phase change in backscattering properties compared to other crops in SAR imaging. As a result, using SAR imaging to monitor rice in foggy areas is highly significant.

erties compared to other crops in SAR imaging. As a result, using SAR imaging to monitor rice in foggy areas is highly significant.

Multi-time-phase SAR imagery, which combines several time-phase SAR images, can accurately depict the changes in rice during the growth cycle and offers more benefits than single-time-phase radar (Neetu & Ray, 2020; Mosleh et al., 2015; Zhang et al., 2020). The most diverse time phases are selected to identify rice from other ground objects based on a comparative analysis of the differences in backscattering strength between rice during the growing period and other ground objects. Nguyen et al. (2016) used time-series dual-polarized (VV/VH) Sentinel-1A Interferometric Wide (IW) images to map rice-planting areas in the Mekong Delta. Bazzi et al. (2019) achieved more than 80% accuracy in mapping rice-planting areas using multi-date Sentinel-1 microwave satellite data. Rice residue burning is a major issue in the western states of India, especially in Haryana and Punjab, during October and November, which also affects the National Capital Region. Rice residue burning generates a large amount of particulate matter and smoke in a short period, raising concerns about public health (Kumar et al., 2015), safety, and the environment. In Punjab, a rice-wheat cropping system is generally followed, resulting in a short sowing window period for farmers to prepare the fields between the rice and wheat crops. Consequently, residue burning becomes an easy practice for farmers to prepare or empty their fields for growing wheat.

n the rice and wheat crops. Consequently, residue burning becomes an easy practice for farmers to prepare or empty their fields for growing wheat.

the rice and wheat crops. Consequently, residue burning becomes an easy practice for farmers to prepare or empty their fields for growing wheat.

Many studies used optical data at a later stage of the crop to identify rice crop areas Jiang et.al. 2016 .Due to cloudy conditions during Kharif rice, availability of cloud free optical data is one of the major limitations. Therefore, multi-date Sentinel-1 microwave satellite data was used for rice crop area identification along with sowing/transplanting date identification in Bathinda, Ludhiana and Gurdaspur districts of Punjab.

## Study Area

Bathinda, Ludhiana, and Gurdaspur are major rice-growing districts in Punjab, covering four different agro-climatic regions: the western plain area, northern plain semiarid, northern plain dry sub-humid, and western Himalayas (Siwalik and Kandi area sub-humid regions) (KVK, Faridkot). Bathinda and Ludhiana districts are situated south of the Sutlej river, known as Malwa, while the Gurdaspur district lies between the Ravi and Beas rivers, known as the Majha region of Punjab. Gurdaspur and Ludhiana are primarily rice-dominant districts, while rice and cotton crops are grown in Bathinda due to water scarcity in the southern and western parts of the district. Figure 1 illustrates the study area.

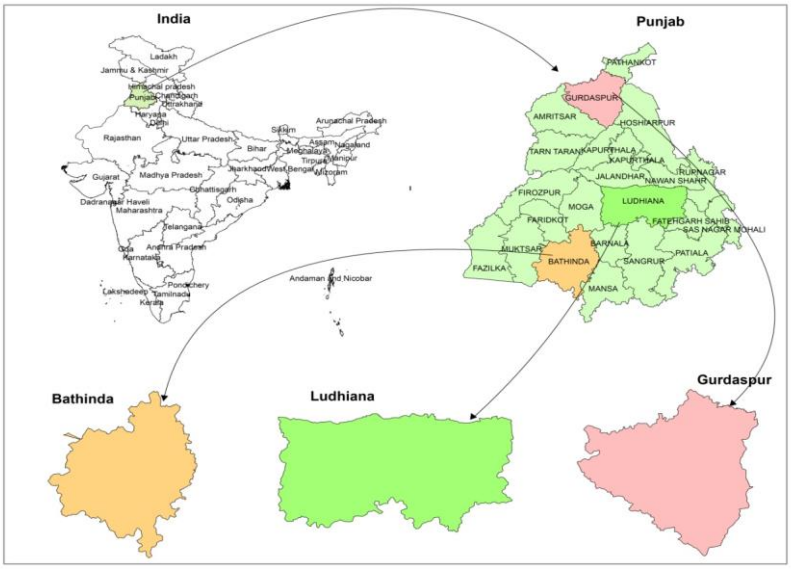


Fig 1. Study Area

## Methodology

### Rice crop identification

Rice is a major kharif crop grown from June to November during India's monsoon season, which makes it challenging to obtain cloud-free optical data (Qadir & Mondal, 2020). Synthetic Aperture Radar (SAR) plays a crucial role in penetrating clouds and providing data in all weather conditions due to its own emitting source and acquisition capabilities (Blaes et al., 2005). Thus, SAR has become a boon for agriculture because of its all-weather data capabilities and polarization sensitivity towards crops. The Sentinel-1 (C-band with a frequency of 5.405 GHz) operates in four different modes: Interferometric Wide Swath Mode (IW), Extra Wide Swath (EW), Strip Map (SM), and Wave Mode (WV). Each mode can produce products at SAR Level-0, Level-1 Single Look Complex (SLC), Level-1 Ground Range Detected (GRD), and Level-2 Ocean (OCN) (ESA, 2013). Interferometric Wide Swath (IW) mode presents a dual-polarization (VH and VV) with a 12-day temporal resolution and a 250 km wide swath (within three sub-swaths) over land at a 5m by 20m spatial resolution (Veloso et al., 2017). The preference for ascending and descending orbits does not significantly affect the ability to differentiate crops (Wood et al., 2002).

ntinel-1 (C-band with a frequency of 5.405 GHz) operates in four different modes: Interferometric Wide Swath Mode (IW), Extra Wide Swath (EW), Strip Map (SM), and Wave Mode (WV). Each mode can produce products at SAR Level-0, Level-1 Single Look Complex (SLC), Level-1 Ground Range Detected (GRD), and Level-2 Ocean (OCN) (ESA, 2013). Interferometric Wide Swath (IW) mode presents a dual-polarization (VH and VV) with a 12-day temporal resolution and a 250 km wide swath (within three sub-swaths) over land at a at a 5m by 20m spatial resolution (Veloso et al., 2017). The preference for ascending and descending orbits does not significantly affect the ability to differentiate crops (Wood et al., 2002).

5m by 20m spatial resolution (Veloso et al., 2017). The preference for ascending and descending orbits does not significantly affect the ability to differentiate crops (Wood et al., 2002).

Lopez Martinez et al. (2018) explained that Level-1 Ground Range Detected (GRD) products consist of focused SAR data that has been detected, multi-looked, and projected to ground range using an Earth ellipsoid model. Sentinel-1 SAR transmits and receives within the C-band microwave region, where interactions are affected by the amount and structure of plant material and ground conditions, such as moisture and surface roughness (Veloso et al., 2017). The vegetation influences the backscatter of VV and VH polarizations, with VV found to be more sensitive to ground conditions (Planque et al., 2021). Freely available multi-date Sentinel-1 SAR data (Spatial Resolution 20m (10*10), Temporal Resolution 12 days, VV polarization, Ground Range Detection Product, high resolution) from 19 May to 15 November for two consecutive years (2019 & 2020) was used for kharif rice classification in the study districts (https://scihub.copernicus.eu/dhus/). Sentinel-1 data has both radiometric and geometric errors due to its slant range viewing angle (20°-46°). Therefore, each scene was preprocessed using Sentinel Application Platform (SNAP) software (ESA, 2017) following the standard procedure of calibration, multi-looking, speckle filtering, terrain correction, and conversion from linear to decibel images.

Calibration converts pixel values to accurately represent SAR backscatter of the reflecting surface, generating sigma naught products (Freeman, 1993). Multi-looking was performed to merge two different resolutions (range and azimuth), enhancing radiometric resolution while decreasing spatial resolution to produce a nominal pixel size (Veloso et al., 2017). SAR images often have a salt-and-pepper effect due to interferences

from atmospheric aerosols, dust particles, and water vapour affecting backscattering radar waves before they reach the SAR instrument. To remove these effects, 2x2 multi-looking was used, which decreases spatial resolution from 10 m to 20 m but increases radiometric resolution. The speckle filter (Bruniquel and Lopes, 1997; Quegan and Yu, 2001) minimizes speckle impact, eliminating the salt-and-pepper effect. The refined Lee filter, known for its ability to preserve edges, linear features, point targets, and texture information, was used as an adaptive filter. Various geometric distortions occur in SAR images due to the side-looking viewing angle and surface topography. To correct each pixel geometrically, the ASTER-1Sec digital elevation model (DEM) was used (Bayanudin & Jatmiko, 2016). Finally, the linear to dB conversion was applied to change the unit-less backscatter coefficient values to dB using a logarithmic conversion.

ous geometric distortions occur in SAR images due to the side-looking viewing angle and surface topography. To correct each pixel geometrically, the ASTER-1Sec digital elevation model (DEM) was used (Bayanudin & Jatmiko, 2016). Finally, the linear to dB conversion was applied to change the unit-less backscatter coefficient values to dB using a logarithmic conversion.

Overall, 12 to 15 successive dates (from 19 May to 15 November) at 12-day temporal resolution were pre-processed, co-registered (geo-registered and mosaicked) to prepare a dataset for the study districts. The rice crop was primarily identified based on flood signal detection from time-series Sentinel-1 microwave data. Therefore, rice identification was carried out using multi-date satellite data and reflected surface backscattering values (Xiao et al., 2021). The classification of rice is a two-step process comprising the selection of optimum dates from the stacked data and the Hierarchical Decision Rule-based Classification (HDRC) model (Jain et al., 2019). Unsupervised (ISODATA) classification was carried out to identify the best date selection, which creates arbitrary clustering based on similar pixels in an image (Ma et al., 2020). A temporal crop profile was plotted to determine the best date selection and the threshold/range of backscattering values for each date. These threshold values were used as input in the HDRC model for rice area identification (Jain et al., 2019).

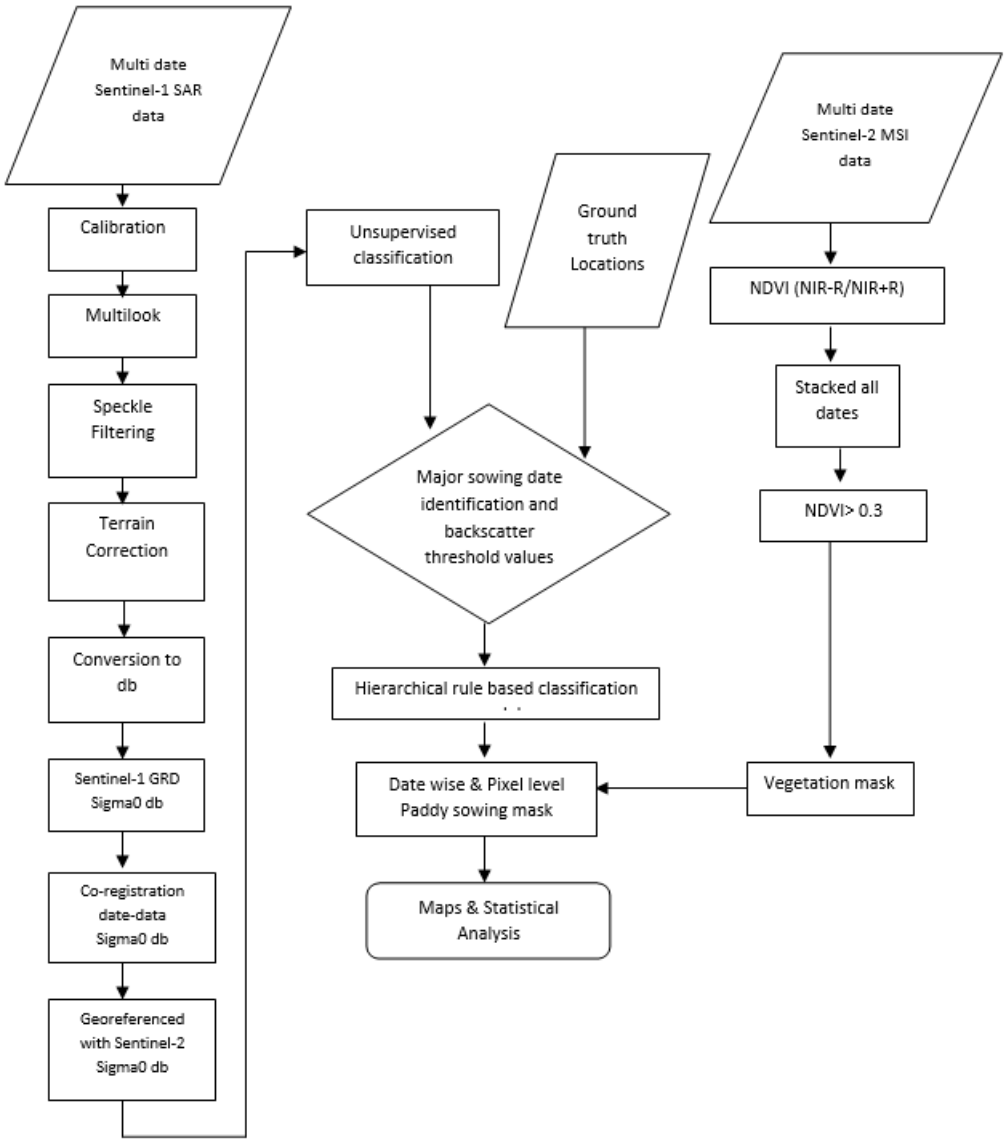


**Fig 2. Flow diagram of methodology**

Typically, fallow land (before rice transplanting) gives higher backscattering (-8 dB to -10 dB) due to surface roughness, while lower backscattering occurs during sowing/transplanting (-17 dB to -19 dB) due to the smooth surface produced by standing water (Jain et al., 2019). As the rice grows, backscattering values increase, reaching around -6 dB to -7 dB at the maximum tillering stage. Other competitive crops like cotton and maize, observed in Bathinda and Gurdaspur districts respectively, grow in dry and moist soil, making it easier to distinguish rice fields from other crops. Hierarchical Rule-based classification was carried out using the selected layers. Typical rice signatures are: $-15 < D1 < -13$, $-12 < D2 < -10$, $-11 < D3 < -8$. Based on this rule-based model, a date-wise kharif rice mask was prepared along with rice area identification, showing the amount of rice sown/transplanted on each satellite date. The land use/land cover classification was carried out using the Normalized Difference Vegetation Index (NDVI) with Landsat-8 satellite data (Song et al., 2019). The NDVI (Sentinel-2 MSI) generated a vegetation mask, which was used to remove non-agricultural pixels from the rice mask. The rice mask was overlaid on the optical image to verify and finalize the classified rice pixels. Ground truth data was collected each year to identify the backscattering values at the time of sowing and to validate the results. The overall accuracy achieved was more than 90% for rice acreage and sowing date identification. The flow diagram showing the overall methodology is presented in Figure 2.
n. The flow diagram showing the overall methodology is presented in Figure 2.

## Results & Discussion

Rice transplantation takes place in standing water, which makes it easier to distinguish from other crops using SAR/microwave satellite data. Multi-date Sentinel-1 SAR data from June to November was used to identify rice crops from other crops for the years 2019 and 2020. The data was corrected both radiometrically and geometrically before classification. The rice crop was classified using a hierarchical rule-based model

based on rice backscatter threshold values, which capture the increasing profile of the crop. Figure 3 shows the growth stages (σ°VV backscatters) of kharif rice for the study area. Low backscattering (-19 to -16 dB) was observed during the sowing/transplantation stage. During the maximum tillering stage, σ°VV backscatters (-13 to -11 dB) gradually increased with rice crop growth. Then, σ°VV backscatter values (around -14 to -15 dB) were observed to decrease in August, likely due to the smooth surface generated by the peak vegetative stage. Two maxima and minima in σ°VV backscatter values were observed during the whole crop period (transplanting to harvesting), followed by an increasing pattern in backscattering from the last week of August at the grain filling stage. The rice crop was separated from other crops like cotton and maize by following these SAR backscatter profiles. Major transplanting dates (12 & 24 June and 6, 18 & 30 July) were observed over the study area.

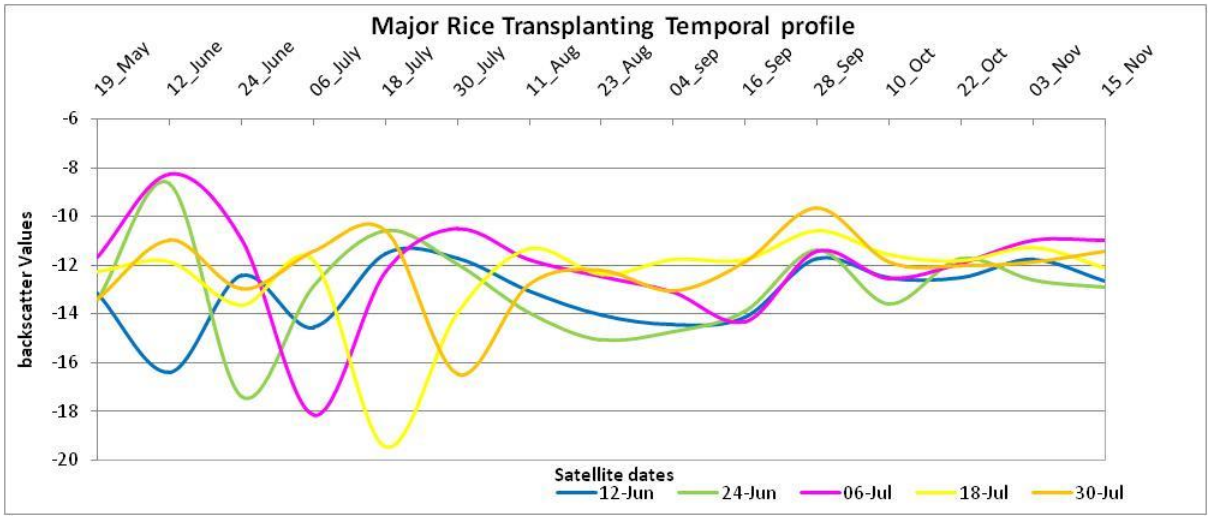


**Fig 3. Rice crop Profile using Sentinel-1 SAR data**

Date-wise sowing/transplanting was classified during rice identification, showing how much rice transplanting (area) took place on particular dates or between dates. The results were then analyzed. Major sowing/transplanting was observed between 12 June and 10 July in all three districts for the years 2019 and 2020. The second fortnight of June was the major sowing/transplanting period in all the districts for both years. Figure 4 shows that sowing/transplanting (%) in all three districts occurred earlier in 2020 compared to 2019, due to the early onset of the monsoon in 2020, verified using rainfall data from the Indian Meteorological Department. It was found that 58.9% (average of 3 districts) of sowing was done in June 2019, while 72.5% (average of 3 districts) was done during the same period in 2020.

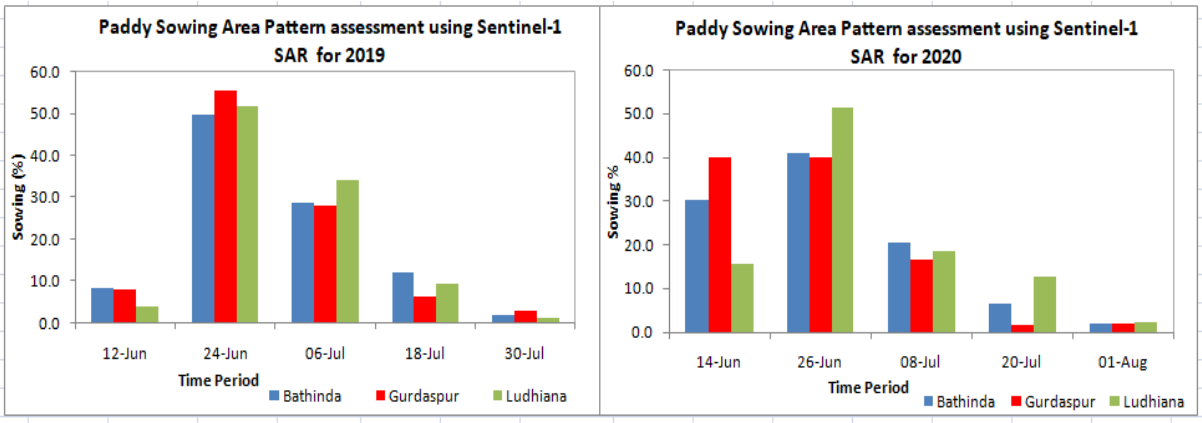


**Fig 4. Rice crop sowing area pattern assessment Sentinel-1 SAR data**

## District wise rice area & Accuracy Assessment

District-wise area was compared with the 3-year average data from the Department of Economics and Statistics (https://www.aps.dac.gov.in/APY/Public_Report1.aspx). Ground truth data was utilized to determine the accuracy parameters for both years. Specifically, both overall accuracy and the user and producer accuracy metrics were calculated. Producer accuracy, which relates to omission errors, indicates the likelihood that a particular class from the ground truth is correctly identified in the classification. In other words, it measures accuracy from the perspective of the data producer, reflecting the proportion of correctly identified instances of each class compared to the total instances of that class in the ground truth. On the other hand, user accuracy addresses commission errors and reflects the likelihood that a class predicted by

the classification corresponds correctly to the actual ground truth. This metric measures accuracy from the perspective of the data user, showing the proportion of correctly classified instances in relation to all instances classified as that particular class. Table 1 below provides the district-wise area comparison and accuracy parameters for both years, offering a detailed comparison of the overall classification performance.
classified instances in relation to all instances classified as that particular class. Table 1 below provides the district-wise area comparison and accuracy parameters for both years, offering a detailed comparison of the overall classification performance.

Table 1 District wise area comparison and accuracy parameters

| | **Area (000ha)** | **DES Avg (000ha)** | **Area (000ha)** | **DES Avg (000ha)** | **Overall Accuracy** | |
|---|---|---|---|---|---|---|
| **District** | **2019** | **(2017-19)** | **2020** | **(2017-19)** | **2019** | **2020** |
| Bathinda | 168.5 | 168.5 | 162.2 | 168.5 | 92% | 91% |
| Ludhiana | 253.1 | 258.6 | 248.2 | 258.6 | 87 % | 89% |
| Gurdaspur | 168.9 | 174.2 | 165.6 | 174.2 | 89% | 87% |

Figures 5 and 6 show the date-wise sowing/transplanting pattern and rice crop area at the pixel level for 2019 and 2020, respectively. In Bathinda, cotton was observed as a competitive crop, whereas sugarcane and maize were reported in the Gurdaspur district. Cotton is grown in the southern part of Bathinda district because the sandy soil in this area, which has high water percolation properties, is not suitable for rice cultivation. In 2019, major transplanting in the Gurdaspur district was observed from the second fortnight of June to the first fortnight of July, whereas in 2020, transplanting occurred earlier (in June) compared to 2019. Early transplantation was also observed in the Ludhiana district in 2020 compared to 2019. The main transplantation period in Ludhiana was from the second fortnight of June to the first fortnight of July for years, 2019 & 2020.

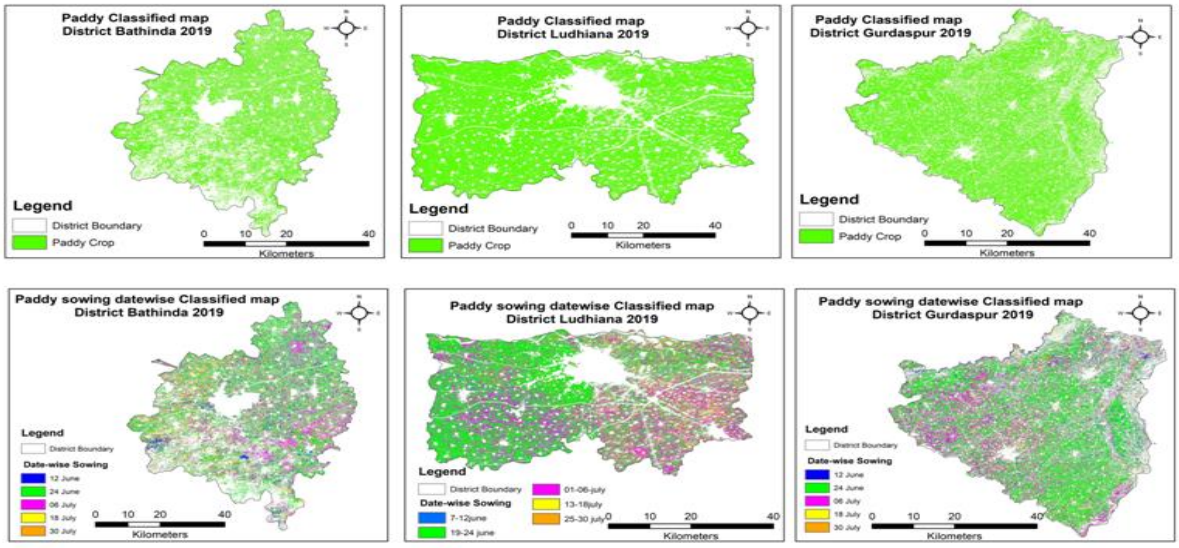


Fig 5. Rice classifid maps for Bathinda,Ludhiana and Gurdaspur districts for 2019

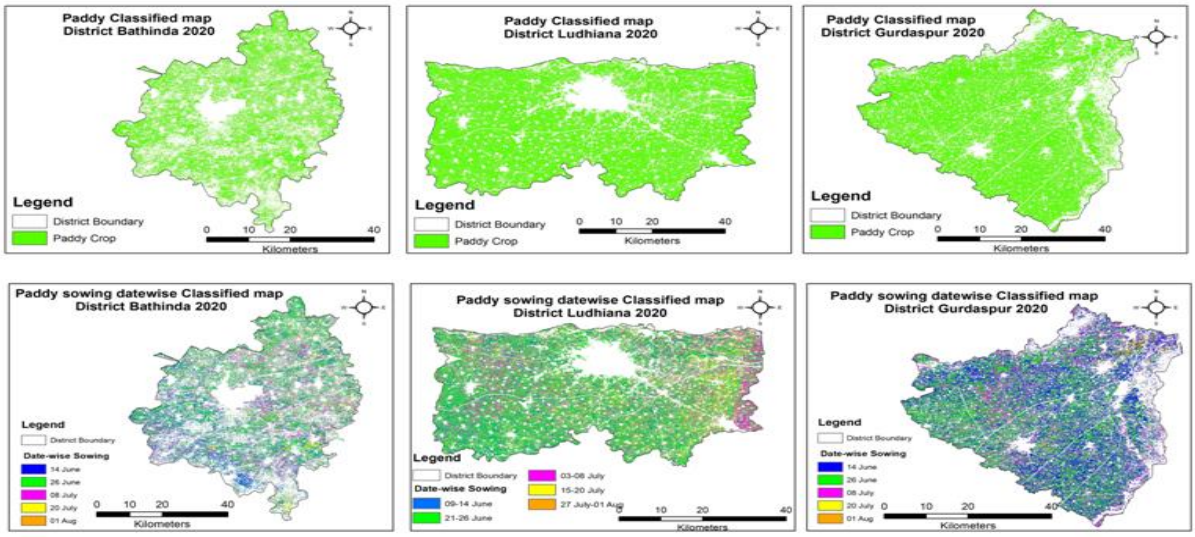


Fig 6. Rice classified maps for Bathinda,Ludhiana and Gurdaspur districts for 2020

## Conclusion

The research effectively utilized Sentinel-1 SAR data to identify rice cultivation areas and delineate sowing dates, especially during the monsoon season when optical data was obscured by cloud cover. Notably, the 2020 season witnessed earlier sowing or transplanting compared to 2019, attributable to the early onset of monsoon that year. The findings suggest that Sentinel-1 SAR adequately assesses the rice crop's area, providing valuable insights for governmental agencies to devise strategies for export and import.

## Reference

1. Bayanudin, A. A., & Jatmiko, R. H. (2016, November). Orthorectification of Sentinel-1 SAR (Synthetic Aperture Radar) Data in Some Parts of South-eastern Sulawesi Using Sentinel-1 Toolbox. In IOP Conference Series: Earth and Environmental Science (Vol. 47, No. 1, p. 012007). IOP Publishing.
2. Bazzi, H., Baghdadi, N., El Hajj, M., Zribi, M., Minh, D. H. T., Ndikumana, E., & Belhouchette, H. (2019). Mapping paddy rice using Sentinel-1 SAR time series in Camargue, France. Remote sensing, 11(7), 887.
3. Blaes, X., Vanhalle, L., & Defourny, P. (2005). Efficiency of crop identification based on optical and SAR image time series. Remote sensing of environment, 96(3-4), 352-365.
4. Boschetti, M., Busetto, L., Manfron, G., Laborte, A., Asilo, S., Pazhanivelan, S., & Nelson, A. (2017). PhenoRice: A method for automatic extraction of spatio-temporal information on rice crops using satellite data time series. Remote sensing of environment, 194, 347-365.
5. Bruniquel, J., & Lopes, A. (1997). Multi-variate optimal speckle reduction in SAR imagery. International journal of remote sensing, 18(3), 603-627.
6. Chen, S. T., Guo, B., Zhang, R., Zang, W. Q., Wei, C. X., Wu, H. W., & Zhang, H. L. (2021). Quantitatively determine the dominant driving factors of the spatial—Temporal changes of vegetation NPP in the Hengduan Mountain area during 2000–2015. Journal of Mountain Science, 18(2), 427-445.
7. ESA, 2017. The Sentinel Application Platform (SNAP), a Common Architecture for all Sentinel Toolboxes Being Jointly Developed by Brockmann Consult, Array Systems Computing and C-S. Downloadable on. http://step.esa.int/main/download/ European. European Space Agency. (2013). Sentinel-1 user handbook [ESA Standard Document]. European Commission, European Union.
8. download/ European. European Space Agency. (2013). Sentinel-1 user handbook [ESA Standard Document]. European Commission, European Union.
9. Freeman, A. (1993). Radiometric calibration of SAR image data. International archives of photogrammetry and remote sensing, 29, 212-212.
10. Government of India (2019). All India crop Situation - kharif 2018-19 as on 27.09.2019.Department of Agriculture, Cooperation and Farmers Welfare, Government of India. Accessed on http://agricoop.nic.in/sites/default/files/Cwwg-data
11. IPCC. Methane Emissions from Rice cultivation: Flooded Rice Fields. In Revised 1996 IPCC Guidelines for National Greenhouse Gas Inventories Refinement; IPCC: Geneva, Switzerland, 1996; Volume 3, pp. 53–75.
12. Jain, V., Saxena, S., Dubey, S., Choudhary, K., Sehgal, S., & Ray, S. S. (2019). Rice (kharif) production estimation using sar data of different satellites and yield models: a comparative analysis of the estimates generated under fasal project. International Archives of the Photogrammetry, Remote Sensing & Spatial Information Sciences.
13. & Spatial Information Sciences.

14. Kumar, P., Kumar, S., & Joshi, L. (2015). Socioeconomic and environmental implications of agricultural residue burning: A case study of Punjab, India (p. 144). Springer Nature.
15. Laborte, A. G., Gutierrez, M. A., Balanza, J. G., Saito, K., Zwart, S. J., Boschetti, M., & Nelson, A. (2017). Rice Atlas, a spatial database of global rice calendars and production. Scientific data, 4(1), 1-10.
16. Li, P., Jiang, L., Feng, Z., Sheldon, S., & Xiao, X. (2016). Mapping rice cropping systems using Landsat-derived renormalized index of normalized difference vegetation index (RNDVI) in the Poyang Lake Region, China. Frontiers of Earth Science, 10, 303-314.
17. Liu, H.Y.; Wang, F.X.; Yang, S.Y (2019). Fast Semi-supervised classification using histogram-based density estimation for large-scale polarimetric SAR data. IEEE Geosci. Remote Sens. Lett. 16, 1844–1848.
18. López-Martínez, C., & MDPI, J. M. L. S. (Eds.). (2018). Polarimetric SAR Techniques and Applications. MDPI.
19. Ma, Z., Liu, Z., Zhao, Y., Zhang, L., Liu, D., Ren, T., & Li, S. (2020). An Unsupervised Crop Classification Method Based on Principal Components Isometric Binning. ISPRS International Journal of Geo-Information, 9(11), 648.
20. Mosleh, M. K., Hassan, Q. K., & Chowdhury, E. H. (2015). Application of remote sensors in mapping rice area and forecasting its production: A review. Sensors, 15(1), 769-791.
21. Neetu, & Ray, S. S. (2020). Evaluation of different approaches to the fusion of Sentinel-1 SAR data and Resourcesat 2 LISS III optical data for use in crop classification. Remote Sensing Letters, 11(12), 1157-1166.
22. Nguyen, D. B., Gruber, A., & Wagner, W. (2016). Mapping rice extent and cropping scheme in the Mekong Delta using Sentinel-1A data. Remote Sensing Letters, 7(12), 1209-1218.
23. Phan, H., Le Toan, T., Bouvet, A., Nguyen, L. D., Pham Duy, T., & Zribi, M. (2018). Mapping of rice varieties and sowing date using X-band SAR data. Sensors, 18(1), 316.
24. Planque, C., Lucas, R., Punalekar, S., Chognard, S., Hurford, C., Owers, C., ... & Bunting, P. (2021). National crop mapping using sentinel-1 time series: A knowledge-based descriptive algorithm. Remote Sensing, 13(5), 846. Jaiswal, Sneha & Jolly, Dr & Kumar, Sumit. (2024).
25. A Comprehensive Analysis of Mahilpur Block's Land Use And Land Cover Using Geospatial Technology. Educational Administration Theory and Practices. 30. 10.53555/kuey.v30i5.2879.
26. Qadir, A., & Mondal, P. (2020). Synergistic Use of Radar and Optical Satellite Data for Improved Monsoon Cropland Mapping in India. Remote Sensing, 12(3), 522.
27. Quegan, S., Yu, J.J., 2001. Filtering of multichannel SAR images. IEEE Trans. Geosci. Remote Sens. 39 (11), 2373–2379.
28. S. Kumar and R. Jolly, "Land Use / Land Cover Change Detection by Multi-Temporal Remote Sensing Imageries: Talwara Block of Punjab, India," Eur. Chem. Bull., vol. 12, no. Special Issue 5, pp. 838–849, 2023.
29. Sishodia R.P., Ray R.L., Singh S.K.(2020) Applications of remote sensing in precision agriculture: A review Remote Sens., 12 (19) (2020), p. 3136.
30. Song, J., Xing, M., Ma, Y., Wang, L., Luo, K., & Quan, X. (2019, July). Crop Classification Using Multitemporal Landsat 8 Images. In IGARSS 2019-2019 IEEE International Geoscience and Remote Sensing Symposium (pp. 2407-2410). IEEE.
31. Ulaby, F. T., Moore, R. K., & Fung, A. K. (1986). Microwave remote sensing: Active and passive. Volume 3-From theory to applications.
32. Veloso, A., Mermoz, S., Bouvet, A., Le Toan, T., Planells, M., Dejoux, J. F., & Ceschia, E. (2017). Understanding the temporal behavior of crops using Sentinel-1 and Sentinel-2-like data for agricultural applications. Remote sensing of environment, 199, 415-426.
33. Wood, D.; McNairn, H.; Brown, R.J.; Dixon, R,(2002). The effect of dew on the use of RADARSAT-1 for crop monitoring: Choosing between ascending and descending orbits. Remote Sens. Environ. 80, 241–247.
34. Xiao, W., Xu, S., & He, T. (2021). Mapping Rice with Sentinel-1/2 and Phenology-, Object-Based Algorithm—A Implementation in Hangjiahu Plain in China Using GEE Platform. Remote Sensing, 13(5), 990.
35. Zhang, Y., Yan, W., Yang, B., Yang, T., & Liu, X. (2020). Estimation of rice yield from a C-band radar remote sensing image by integrating a physical scattering model and an optimization algorithm. Precision Agriculture, 21, 245-263.